PHYSICAL REVIEW D **88,** 033007 (2013)

Weak radiative pion vertex in $\tau^- \to \pi^- \nu_\tau \ell^+ \ell^-$ decays

P. Roig,[1] A. Guevara,[2] and G. López Castro[2]

[1]*Grup de Física Teòrica, Institut de Física d'Altes Energies, Universitat Autònoma de Barcelona, E-08193 Bellaterra, Barcelona, Spain*

[2]*Departamento de Física, Centro de Investigación y de Estudios Avanzados, Apartado Postal 14-740, 07000 México D.F., México*

(Received 12 June 2013; published 19 August 2013)

We carry out a detailed study of the branching fractions and lepton-pair invariant-mass spectrum of $\tau^- \to \pi^- \nu_\tau \ell^+ \ell^-$ decays ($\ell = e,\ \mu$). In addition to the model-independent (QED) contributions, we include the structure-dependent (SD) terms, which encode information on the hadronization of QCD currents. The form factors describing the SD contributions are evaluated by supplementing Chiral Perturbation Theory with the inclusion of the lightest multiplet of spin-1 resonances as active degrees of freedom. The Lagrangian couplings have been determined by demanding the known QCD short-distance behavior to the relevant Green functions and associated form factors in the limit where the number of colors goes to infinity. As a result, we predict $\mathrm{BR}(\tau^- \to \pi^- \nu_\tau e^+ e^-) = (1.7^{+1.1}_{-0.3}) \times 10^{-5}$ and $\mathrm{BR}(\tau^- \to \pi^- \nu_\tau \mu^+ \mu^-) \in [0.03, 1.0] \times 10^{-5}$. According to this, the first decay could be measured in the near future, which is not granted for the second one.

DOI: 10.1103/PhysRevD.88.033007 PACS numbers: 13.35.Dx, 12.39.Fe, 12.38.−t

I. INTRODUCTION

The hadronic final states that can be produced in τ-lepton decays provide a clean environment to study the dynamics of strong interactions at energies below the τ-lepton mass. The leading weak interactions that drive the flavor transitions in these decays are dressed by the strong and electromagnetic interactions to generate a large diversity of hadronic and photonic states. The hadronic vertices can be cleanly extracted and used to test several properties of QCD and electroweak interactions, or to extract fundamental parameters of the Standard Model [1].

In this paper, we study the $\tau^\pm \to \pi^\pm \nu_\tau \ell^+ \ell^-$ ($\ell = e$ or μ) decays, which have been considered previously [2] in the context of sterile neutrino exchange. The calculation in Ref. [2] overlooks the Standard Model contribution which, to our knowledge, has not been studied before and it is tackled for the first time in the present paper. We will present the results of this calculation and analyze the associated phenomenology in this article, ignoring all possible new physics contributions. The attempt to measure these decay channels has not been made so far, although, as we will show, they are likely to be detected in near-future facilities. The τ-lepton decays under consideration are the crossed channels of the $\pi^\pm \to \ell^\pm \nu_\ell e^+ e^-$ decays, which have been studied in the past [3,4] and have been already observed [5]. Both decays are interesting because they involve the $\gamma^* W^{*\mp} \pi^\pm$ vertex with the two gauge bosons off their mass shells. The analogous radiative $\tau^\pm \to \pi^\pm \nu_\tau \gamma$ and $\pi^\pm \to \ell^\pm \nu_\ell \gamma$ decays, which have been widely studied before [6–9], provide information on the same vertex in the case of a real photon. The knowledge of the $\gamma W \pi$ vertex in the full kinematical range is of great importance, not only for testing QCD predictions, but also because it plays a relevant role in computing the radiative corrections to $\pi \to \ell \nu$, $\tau \to \pi \nu_\tau$ decays and in the evaluation of the hadronic light-by-light contributions to the muon anomalous magnetic moment [10].

These four-body decays of pions and τ leptons explore different virtualities of the photon and W boson and can provide complementary information on the relevant form factors. The low energies involved in pion decays are sensitive to QCD predictions in the chiral and isospin limits, while τ-lepton decays involve energy scales where the resonance degrees of freedom become relevant. As is well known, rigorous predictions from QCD for the form factors that describe the $\gamma W \pi$ and $\gamma\gamma\pi$ vertices can be obtained only in the chiral and short-distance limits. Therefore, the information provided by τ-lepton decays is valuable in order to understand the extrapolation between these two limiting cases.

The vector and axial-vector form factors relevant to our study are calculated in the framework of the Resonance Chiral Theory (RχT) [11,12]. In order to fix the free couplings appearing in these calculations, we also impose available short-distance constraints in the large-N_C limit of QCD. As a result, we are able to predict the branching ratios and the invariant-mass spectrum of the lepton pair in $\tau^\pm \to \pi^\pm \nu_\tau \ell^+ \ell^-$ decays.

In Sec. II, we decompose the matrix element in terms of the model-independent (QED) and the structure-dependent (SD; vector and axial-vector) contributions, where the latter depend on the corresponding hadronic form factors. These are studied in detail in Sec. III, and the QCD constraints on their short-distance behavior in the $N_C \to \infty$ limit are discussed in Sec. IV. The related phenomenological analysis is presented in Sec. V, and we give our conclusions in Sec VI. An appendix with the results of the spin-averaged squared matrix element completes our discussion.

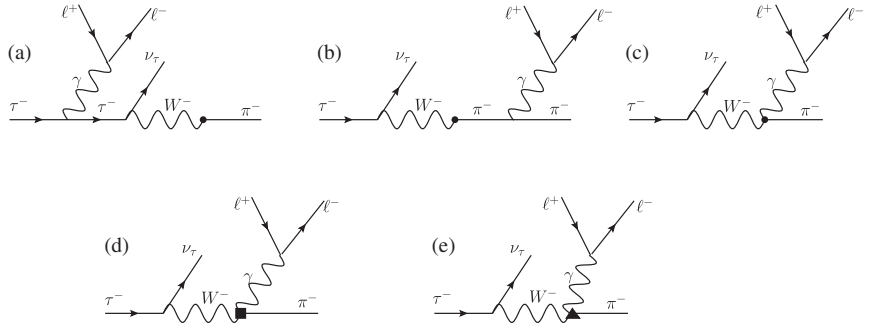

FIG. 1. Feynman diagrams for the different kinds of contributions to the $\tau^- \to \pi^- \nu_\tau \ell^+ \ell^-$ decays, as explained in the main text. The dot indicates the hadronization of the QCD currents. The solid triangle (square) represents the SD contribution mediated by the axial-vector (vector) current.

II. MATRIX ELEMENT AND DECAY RATE

We consider the process $\tau^-(p_\tau) \to \pi^-(p)\nu_\tau(q) \times \ell^+(p_+)\ell^-(p_-)$. This decay is generated by demanding that the photon in the $\tau^-(p_\tau) \to \pi^-(p)\nu_\tau(q)\gamma(k)$ decays become virtual and then convert into a lepton pair (lepton-pair production mediated by the Z boson is negligible); at the amplitude level, it suffices to change the photon polarization ϵ^μ in the radiative decay by $e\bar{u}(p_-)\gamma_\mu \times v(p_+)/k^2$, with $k = p_+ + p_-$ the photon momentum and e the positron charge. Therefore, one can relate the description of the structure-dependent contributions to lepton-pair production to the ones appearing in the real photon case [9]. In analogy with the radiative pion and one-meson tau decays, the matrix element can be written as the sum of four contributions:

$$\mathcal{M}[\tau^-(p_\tau) \to \pi^-(p)\nu_\tau(q)\ell^+(p_+)\ell^-(p_-)] = \mathcal{M}_{IB_\tau} + \mathcal{M}_{IB_\pi} + \mathcal{M}_V + \mathcal{M}_A. \quad (1)$$

The relevant diagrams are depicted in Fig. 1. The notation introduced for the amplitudes describes the four kinds of contributions: $\mathcal{M}_{IB_\tau}$ is the bremsstrahlung off the tau lepton, [Fig. 1(a)]; $\mathcal{M}_{IB_\pi}$ is the sum of the bremsstrahlung off the π meson [Fig. 1(b)] and the diagram with the local $W^*\gamma^*\pi$ vertex [Fig. 1(c)]; $\mathcal{M}_V$ is the structure-dependent vector contribution [Fig. 1(d)]; and $\mathcal{M}_A$ is the structure-dependent axial-vector contribution [Fig. 1(e)]. Our imprecise knowledge of the exact mechanism of hadronization in the last two terms is parametrized in terms of hadronic form factors, which are functions of $p \cdot k$ and k^2.

The decay amplitude is composed of the following set of gauge-invariant contributions (G_F is the Fermi constant, $V_{ud} = 0.9742$ the ud quark mixing angle, $F_\pi = 92.2$ MeV [5], and we have defined $\mathcal{M}_{IB} = \mathcal{M}_{IB_\tau} + \mathcal{M}_{IB_\pi}$):

$$\begin{aligned}
\mathcal{M}_{IB} &= -iG_F V_{ud}\frac{e^2}{k^2}F_\pi M_\tau \bar{u}(p_-)\gamma_\mu v(p_+)\bar{u}(q)(1+\gamma_5)\left[\frac{2p^\mu}{2p\cdot k + k^2} + \frac{2p_\tau^\mu - \not{k}\gamma^\mu}{-2p_\tau\cdot k + k^2}\right]u(p_\tau),\\
\mathcal{M}_V &= -G_F V_{ud}\frac{e^2}{k^2}\bar{u}(p_-)\gamma^\nu v(p_+)F_V(p\cdot k, k^2)\epsilon_{\mu\nu\rho\sigma}k^\rho p^\sigma \bar{u}(q)\gamma^\mu(1-\gamma_5)u(p_\tau),\\
\mathcal{M}_A &= iG_F V_{ud}\frac{2e^2}{k^2}\bar{u}(p_-)\gamma_\nu v(p_+)\Big\{F_A(p\cdot k, k^2)[(k^2 + p\cdot k)g^{\mu\nu} - k^\mu p^\nu] - \frac{1}{2}A_2(k^2)k^2 g^{\mu\nu}\\
&\quad + \frac{1}{2}A_4(k^2)k^2(p+k)^\mu p^\nu\Big\}\bar{u}(q)\gamma_\mu(1-\gamma_5)u(p_\tau). \quad (2)
\end{aligned}$$

The structure-dependent contributions are described in terms of one vector and three axial-vector Lorentz-invariant form factors. These form factors will be discussed in detail later in the article and, in particular, the dependence on k^2 of $F_A(p\cdot k, k^2)$ and $F_V(p\cdot k, k^2)$ will be given in Sec. III. It can be easily checked that the decay amplitudes corresponding to the radiative $\tau^- \to \pi^-\nu_\tau\gamma$ decays can be obtained from Eq. (2) by replacing $e\bar{u}(p_-)\gamma^\mu v(p_+) \to \epsilon^\mu/k^2$, where ϵ^μ is the polarization four-vector of the real photon, and then by setting $k^2 = 0$. In this case, the decay amplitude depends only upon two form factors, $F_A(p\cdot k, k^2 = 0)$ and $F_V(p\cdot k, k^2 = 0)$, whose expressions can be read from Ref. [9]. The additional axial-vector form factors $A_2(k^2)$ and $A_4(k^2)$ can be found in Ref. [6].

Equation (2) can be checked from the corresponding expressions for $K^+ \to \mu^+\nu_\mu\ell^+\ell^-$ in Eq. (4.9) of Ref. [6] by using crossing symmetry and the conservation of the electromagnetic current. As noted in this reference, the parametrization of the axial-vector form factor used by

the Particle Data Group [5] for the analogous $\pi^+ \to \mu^+ \nu_\mu e^+ e^-$ decays neglects the $A_4(k^2)$ form factor.[1] Given the different kinematics of our problem, we will keep it in the following. As we will see later, at next-to-leading order in Chiral Perturbation Theory (χPT), $A_2(k^2)$ and $A_4(k^2)$ can be expressed in terms of only one form factor. (This is no longer true at the next order [6], whose contributions we neglect.) If we define this form factor as $B(k^2) \equiv -\frac{1}{2}A_2(k^2)$, then $\frac{1}{2}A_4(k^2) = -B(k^2)/(k^2 + 2p\cdot k)$, and the axial-vector SD amplitude is simplified to

$$\begin{aligned}\mathcal{M}_A = {} & iG_F V_{ud}\frac{2e^2}{k^2}\bar{u}(p_-)\gamma_\nu v(p_+) \\ & \times \Big\{F_A(p\cdot k, k^2)[(k^2 + p\cdot k)g^{\mu\nu} - k^\mu p^\nu] \\ & + B(k^2)k^2\Big[g^{\mu\nu} - \frac{(p+k)^\mu p^\nu}{k^2 + 2p\cdot k}\Big]\Big\} \\ & \times \bar{u}(q)\gamma_\mu(1-\gamma_5)u(p_\tau). \end{aligned} \tag{3}$$

The results of summing the different contributions to the squared matrix element over polarizations are collected in the Appendix.

The IB contributions are model independent in the sense that they are determined in terms of the parameters of the well-known nonradiative $\tau^- \to \pi^- \nu_\tau$ decays and by using QED. They provide the dominant contribution to the decay rate in the case of a real photon emission [9], owing to the well-known infrared divergent behavior. For the decay under consideration, we can expect that this behavior is softened, since $k^2 \geq 4m_\ell^2$. The SD (or model-dependent) contributions require the modeling of the $\gamma^* W^* \pi$ vertex for photon and W-boson virtualities of the order of 1 GeV. Those terms can be split into vector V and axial-vector A contributions, according to Eq. (2), and must include the resonance degrees of freedom that are relevant at such energies (see Sec. III).

Therefore, the decay rate can be conveniently separated into six terms which correspond to three moduli squared (IB, VV, AA) and three interference terms ($IB - V$, $IB - A$, $V - A$). Thus, we can write the decay rate as follows:

$$\Gamma_{\text{total}} = \Gamma_{IB} + \Gamma_{VV} + \Gamma_{AA} + \Gamma_{IB-V} + \Gamma_{IB-A} + \Gamma_{V-A}. \tag{4}$$

In terms of the five independent kinematical variables needed to describe a four-body decay, the differential decay rate is given by

$$\begin{aligned} & d\Gamma(\tau^- \to \nu_\tau \pi^- \ell^+ \ell^-) \\ & \quad = \frac{X\beta_{12}\beta_{34}}{4(4\pi)^6 M_\tau^3}\overline{|\mathcal{M}|^2} ds_{34} ds_{12} d(\cos\theta_1) d(\cos\theta_3) d\phi_3, \end{aligned} \tag{5}$$

where $\overline{|\mathcal{M}|^2}$ is the spin-averaged unpolarized decay probability,

$$X = \frac{\lambda^{1/2}(M_\tau^2, s_{12}, s_{34})}{2}, \qquad \beta_{ij} = \frac{\lambda^{1/2}(s_{ij}, m_i^2, m_j^2)}{s_{ij}}, \tag{6}$$

and $\lambda(a,b,c) = a^2 + b^2 + c^2 - 2ab - 2ac - 2bc$.

The five independent kinematical variables in Eq. (5) were chosen as $\{s_{12}, s_{34}, \theta_1, \theta_3, \phi_3\}$, where $s_{12} := (p_1 + p_2)^2$ and $s_{34} := (p_3 + p_4)^2$; the momenta were relabeled[2] as

$$\{p_\tau, q, p, p_+, p_-\} \to \{p, p_1, p_2, p_3, p_4\}. \tag{7}$$

The definition of the angles is the standard one. Finally, the integration limits are

$$\begin{aligned} & s_{34}^{\min} = (m_3 + m_4)^2, \qquad s_{34}^{\max} = (M - m_1 - m_2)^2, \\ & \qquad \theta_{1,3} \in [0, \pi], \qquad \phi_3 \in [0, 2\pi], \\ & s_{12}^{\min} = (m_1 + m_2)^2, \qquad s_{12}^{\max} = (M - \sqrt{s_{34}})^2. \end{aligned} \tag{8}$$

In this way, the outermost integration corresponds to the square of the invariant mass s_{34} of the lepton-antilepton pair, assuming it can be the spectrum most easily measured in the considered decays.

III. STRUCTURE-DEPENDENT FORM FACTORS

Although the hadronic form factors cannot be computed from the underlying theory, the symmetries of QCD are nonetheless the guiding principle for writing the effective Lagrangian that will be used. At very low energies, the strong-interaction Lagrangian exhibits a chiral $SU(n_f) \otimes SU(n_f)$ symmetry in the approximate limit of (n_f) massless light quarks. This symmetry allows us to develop χPT [14] as an expansion in powers of momenta and masses of the lightest mesons (that acquire mass through explicit chiral symmetry breaking), over a typical hadronic scale which can be identified with the lightest resonances or the chiral symmetry breaking scale. Since the energies probed in hadronic tau decays are larger than these hadronic scales, the χPT expansion parameter no longer converges at high invariant masses. In parallel new degrees of freedom, the lightest resonances become excited, and they should be introduced as dynamical fields in the action. This is done in RχT [11], working in the convenient antisymmetric tensor formalism, which guarantees that the contact interactions of next-to-leading order (NLO) χPT are already included in the RχT Lagrangian, as can be seen by integrating the resonances out. Now the expansion parameter is $1/N_C$ (N_C being the number of

[1] The other form factors are related via $-\sqrt{2}m_\pi[F_A(p\cdot k, k^2), A_2(k^2), F_V(k^2)] = [F_A, R, F_V]$ to the ones used in Ref. [5].

[2] We decided to write Eqs. (5) and (6) in terms of the second set of momenta in Eq. (7) for its general usefulness in four-body decays. See Ref. [13] for details. By contrast, we prefer to present the rest of Eq. (1) to Eq. (A2) in terms of the first set of momenta in Eq. (7) for an easier interpretation.

FIG. 2. Vector current contributions to the $W^{-*} \to \pi^- \gamma^*$ vertex.

FIG. 3. Axial-vector current contributions to the $W^{-*} \to \pi^- \gamma^*$ vertex.

colors of the gauge group) [15], and the theory at leading order has a spectrum of infinitely many stable states with only tree-level interactions. In our case, we will see that the kinematics of the problem damps very strongly the observables above 1 GeV, which justifies considering only the exchange of the lightest vector and axial-vector resonance multiplets.[3] We will introduce the most important NLO correction in the $1/N_C$ counting given by the meson widths, as they are needed to achieve a sensible description of the propagating resonances.

The relevant effective Lagrangian reads as follows:

$$\begin{aligned}\mathcal{L}_{\mathrm{R}\chi\mathrm{T}} \doteq\ & \mathcal{L}_{WZW} + \mathcal{L}^{\mathrm{V}}_{\mathrm{kin}} + \frac{F_\pi^2}{4}\langle u_\mu u^\mu + \chi_+\rangle \\ & + \frac{F_V}{2\sqrt{2}}\langle V_{\mu\nu} f_+^{\mu\nu}\rangle + i\frac{G_V}{\sqrt{2}}\langle V_{\mu\nu} u^\mu u^\nu\rangle \\ & + \sum_{i=1}^{7}\frac{c_i}{M_V}\mathcal{O}^i_{\mathrm{VJP}} + \sum_{i=1}^{4} d_i \mathcal{O}^i_{\mathrm{VVP}} + \sum_{i=1}^{5}\lambda_i \mathcal{O}^i_{\mathrm{VAP}}, \end{aligned} \tag{9}$$

where all coupling constants are real and M_V is the mass of the lightest vector meson resonance nonet [16]. We follow here the notation in Refs. [11,17,18], where the explicit form of these operators can be found.

The structure-dependent form factors in $\tau^- \to \nu_\tau \pi^- \ell^+ \ell^-$ decays that appear in Eq. (2) can be obtained from the same Feynman diagrams considered in Ref. [9] for the $\tau^- \to \nu_\tau \pi^- \gamma$ decays. This is achieved by replacing the real photon with a virtual one, which then converts into the lepton-antilepton pair. These diagrams are given in Figs. 2 and 3 for the vector and axial-vector current contributions, respectively.

Since both the W gauge boson and the photon are virtual in the present case, the form factors defining the $\gamma^* W^* \pi$ vertex will depend upon two invariant variables, which we choose as $t := (p+k)^2 = k^2 + 2p\cdot k + m_\pi^2$ and k^2. The other important difference is that the second diagram of Fig. 3—which was zero for real photons [9]—will now contribute, giving rise to the additional form factor $B(k^2)$. This term can be related to the isovector component of the electromagnetic $\pi^+\pi^-$ form factor [6], and it accounts for the off-shell-ness of the photon that is not contained in the pure QED contribution.

In the framework of the RχT, the vector form factor $F_V(t, k^2)$, defined in Eq. (2), adopts the following expression:

$$\begin{aligned} F_V(t,k^2) =\ & -\frac{N_C}{24\pi^2 F_\pi} + \frac{2\sqrt{2}F_V}{3F_\pi M_V}[(c_2 - c_1 - c_5)t + (c_5 - c_1 - c_2 - 8c_3)m_\pi^2 \\ & + 2(c_6 - c_5)k^2]\left[\frac{\cos^2\theta}{M_\phi^2 - k^2 - iM_\phi\Gamma_\phi}(1 - \sqrt{2}\mathrm{tg}\theta) + \frac{\sin^2\theta}{M_\omega^2 - k^2 - iM_\omega\Gamma_\omega}(1 + \sqrt{2}\mathrm{cotg}\theta)\right] \\ & + \frac{2\sqrt{2}F_V}{3F_\pi M_V} D_\rho(t)[(c_1 - c_2 - c_5 + 2c_6)t + (c_5 - c_1 - c_2 - 8c_3)m_\pi^2 + (c_2 - c_1 - c_5)k^2] \\ & + \frac{4F_V^2}{3F_\pi} D_\rho(t)[d_3(t + 4k^2) + (d_1 + 8d_2 - d_3)m_\pi^2]\left[\frac{\cos^2\theta}{M_\phi^2 - k^2 - iM_\phi\Gamma_\phi}(1 - \sqrt{2}\mathrm{tg}\theta)\right. \\ & \left. + \frac{\sin^2\theta}{M_\omega^2 - k^2 - iM_\omega\Gamma_\omega}(1 + \sqrt{2}\mathrm{cotg}\theta)\right], \end{aligned} \tag{10}$$

where

[3]Given the (axial-)vector character of the Standard Model couplings of the hadronic matrix elements in τ decays, form factors for these processes are ruled by vector and axial-vector resonances.

$$D_\rho(t) = \frac{1}{M_\rho^2 - t - iM_\rho \Gamma_\rho(t)} \tag{11}$$

and $\Gamma_\rho(t)$ stands for the decay width of the $\rho(770)$ resonance included, following the definition given in Ref. [19]:

$$\Gamma_\rho(s) = \frac{sM_\rho}{96\pi F_\pi^2}\left[\sigma_\pi^3(s)\theta(s-4m_\pi^2) + \frac{1}{2}\sigma_K^3(s)\theta(s-4m_K^2)\right], \tag{12}$$

with $\sigma_P(s) = \sqrt{1-\frac{4m_P^2}{s}}$.

For the purposes of numerical evaluation, we will assume the ideal mixing for the $\omega - \phi$ system of vector resonances, namely

$$\begin{aligned}\omega_1 &= \cos\theta\omega - \sin\theta\phi \sim \sqrt{\frac{2}{3}}\omega - \sqrt{\frac{1}{3}}\phi,\\ \omega_8 &= \sin\theta\omega + \cos\theta\phi \sim \sqrt{\frac{2}{3}}\phi + \sqrt{\frac{1}{3}}\omega.\end{aligned} \tag{13}$$

In this limit, the contribution of the ϕ meson to Eq. (10) vanishes; in addition, we will neglect any energy dependence in their off-shell widths, given that they are rather narrow resonances.

Similarly, the axial-vector form factor $F_A(t,k^2)$ is given by

$$\begin{aligned}F_A(t,k^2) = {}& \frac{F_V^2}{F_\pi}\left(1 - \frac{2G_V}{F_V}\right)D_\rho(k^2) - \frac{F_A^2}{F_\pi}D_{a_1}(t)\\ &+ \frac{F_A F_V}{\sqrt{2}F_\pi}D_\rho(k^2)D_{a_1}(t)(-\lambda'' t + \lambda_0 m_\pi^2),\end{aligned} \tag{14}$$

where we have used the notation

$$\begin{aligned}\sqrt{2}\lambda_0 &= -4\lambda_1 - \lambda_2 - \frac{\lambda_4}{2} - \lambda_5,\\ \sqrt{2}\lambda'' &= \lambda_2 - \frac{\lambda_4}{2} - \lambda_5\end{aligned} \tag{15}$$

for the relevant combinations of the couplings in $\mathcal{L}_2^{\rm VAP}$ [Eq. (9)].

The energy-dependent $a_1(1260)$ resonance width entering $D_{a_1}(t)$ was studied within this framework in Ref. [20], where the dominant $\pi\pi\pi$ and $KK\pi$ absorptive cuts where obtained in terms of the corresponding three-meson form factors [20,21]. Here we have used the updated fit results of Ref. [22], which were obtained using the complete multidimensional distributions measured by *BABAR* [23].

Finally, the additional axial-vector form factor $B(k^2)$ is

$$B(k^2) = F_\pi \frac{F_V^{\pi^+\pi^-}|_\rho(k^2) - 1}{k^2}, \tag{16}$$

where $F_V^{\pi^+\pi^-}|_\rho$ corresponds to the $I=1$ part of the $\pi^+\pi^-$ vector form factor. Based on the effective field theory description of Ref. [24] including only the $\rho(770)$ contribution and reproducing the χPT results [25–27], several phenomenological approaches including the effect of higher excitations have been developed [28,29]. This form factor has also been addressed within dispersive representations exploiting analyticity and unitarity constraints [30–33]. Here we will follow the approach of Ref. [34] and will use a dispersive representation of the form factor at low energies matched to a phenomenological description at intermediate energies, including the excited resonances contribution. A three-times subtracted dispersion relation will be used:

$$F_V^\pi(s) = \exp\left[\alpha_1 s + \frac{\alpha_2}{2}s^2 + \frac{s^3}{\pi}\int_{s_{\rm thr}}^\infty ds' \frac{\delta_1^1(s')}{(s')^3(s'-s-i\epsilon)}\right], \tag{17}$$

where [35]

$$\tan\delta_1^1(s) = \frac{\Im m F_V^{\pi(0)}(s)}{\Re e F_V^{\pi(0)}(s)} \tag{18}$$

with

$$F_V^{\pi(0)}(s) = \frac{M_\rho^2}{M_\rho^2[1 + \frac{s}{96\pi^2F_\pi^2}(A_\pi(s) + \frac{1}{2}A_K(s))] - s} = \frac{M_\rho^2}{M_\rho^2[1 + \frac{s}{96\pi^2F_\pi^2}\Re e(A_\pi(s) + \frac{1}{2}A_K(s))] - s - iM_\rho\Gamma_\rho(s)}. \tag{19}$$

The loop function is (μ can be taken as M_ρ)

$$A_P(k^2) = \ln\left(\frac{m_P^2}{\mu^2}\right) + 8\frac{m_P^2}{k^2} - \frac{5}{3} + \sigma_P^3(k^2)\ln\left(\frac{\sigma_P(k^2)+1}{\sigma_P(k^2)-1}\right), \tag{20}$$

and the phase-space factor $\sigma_P(k^2)$ was defined after Eq. (12).

The parameters α_1, α_2 and the $\rho(770)$ resonance parameters entering $B(k^2)$ will be extracted [34] from fits to *BABAR* $\sigma(e^+e^- \to \pi^+\pi^-)$ data [36], excluding the $\omega(782)$ contribution. We have used the preliminary values $\alpha_1 = 1.87$, $\alpha_2 = 4.26$ in the numerics.

IV. SHORT-DISTANCE CONSTRAINTS

The form factors derived in the previous section satisfy the constraints imposed by chiral symmetry. Some of the remaining free parameters can be fixed by requiring that they satisfy the short-distance QCD behavior. The study of two-point spin-1 Green functions within perturbative QCD [37] shows that both of them go to a constant value at infinite transfer of momenta. Assuming local duality, the imaginary part of the quark loop can be understood as the sum of infinite positive contributions of intermediate hadron states. If these must add up to a constant, it should be expected that each of the contributions vanishes in that

limit. This vanishing should be accomplished asymptotically and, consequently, it is expected that all resonance excitations up to the QCD continuum contribute to the meson form factors in this limit. This conclusion is also derived from the large-N_C limit of QCD, where these requirements find their most natural application.

On the contrary, phenomenology suggests that the effect of excited resonances on the short-distance relations is pretty small. To give just two examples, if the effects of the $\rho(1450)$ resonance are ignored in the pion vector form factor [24], the generic asymptotic constraint (where i corresponds to the index of the multiplet)

$$\sum_i F_V^i G_V^i = F_\pi^2 \tag{21}$$

that is obtained in the $N_C \to \infty$ limit reduces to $F_V G_V = F_\pi^2$. Upon integration of the resonances, this produces the prediction of the χPT low-energy coupling,

$$L_9 = \frac{F_V G_V}{2M_\rho^2} = \frac{F_\pi^2}{2M_\rho^2} = 7.2 \times 10^{-3}, \tag{22}$$

in remarkably good agreement with the phenomenologically extracted value, which shows that the corrections to obtaining the high-energy constraint considering only the lightest multiplet are smaller than 5% in this case.

Our second example concerns the study of the $\tau^- \to (K\pi)^- \nu_\tau$ decays. In Ref. [38], the effect of the $K^\star(1410)$ resonance was included through

$$\gamma = -\frac{F_V' G_V'}{F^2} = \frac{F_V G_V}{F^2} - 1. \tag{23}$$

While $\gamma = 0$ if the second multiplet is neglected, in the subsequent analyses [35,39,40] it was found to be $\gamma = -0.05 \pm 0.02$, which supports the idea that the modifications introduced by the second multiplet to the short-distance constraints are at the 5% level.[4]

This number should be, however, enlarged for estimating the error associated with the neglect of the heavier multiplets on the high-energy constraints in our problem. The previous examples were given for two-meson form factors, and we are dealing with the form factors corresponding to (axial-vector) current coupled to a pseudoscalar and a photon (giving the lepton-antilepton pair), which has a much richer dynamics. Our estimate on the error is discussed at the end of this section.

The vanishing of the vector form factor in Eq. (10) for $t \to \infty$ and $k^2 \to \infty$ yields

$$c_1 - c_2 + c_5 = 0, \qquad 2(c_6 - c_5) = \frac{-N_C M_V}{32\sqrt{2}\pi^2 F_V}, \tag{24}$$

in agreement with the results of Ref. [17] for the VVP Green's function. No restrictions are found on the other couplings entering Eq. (10). The high-energy conditions found in Ref. [17] for them are

$$\begin{aligned} -c_1 - c_2 - 8c_3 + c_5 &= 0, \\ d_1 + 8d_2 - d_3 &= \frac{F_\pi^2}{8F_V^2}, \\ d_3 &= \frac{-N_C}{64\pi^2}\frac{M_V^2}{F_V^2} + \frac{F_\pi^2}{8F_V^2}. \end{aligned} \tag{25}$$

No short-distance requirements are obtained for the axial-vector form factor in Eq. (14), which already vanishes in the limit of k^2 and t simultaneously large. The corresponding couplings are constrained by the high-energy conditions on the two-point Green functions of vector and axial-vector currents [11]:

$$F_V G_V = F_\pi^2, \qquad 2F_V G_V - F_V^2 = 0, \tag{26}$$

and by the short-distance constraints applying in the VAP Green's function [42] and three-meson hadronic form factors [20,21]:

$$\lambda' = \frac{F_\pi^2}{2\sqrt{2}F_A G_V}, \qquad \lambda'' = \frac{2G_V - F_V}{2\sqrt{2}F_A}, \qquad \lambda_0 = \frac{\lambda' + \lambda''}{4}. \tag{27}$$

If the Weinberg sum rules [43] ($F_V^2 - F_A^2 = F_\pi^2$, $F_V^2 M_V^2 = F_A^2 M_A^2$) are imposed, all couplings are predicted in terms of F_π and M_V:

$$\begin{aligned} c_1 - c_2 + c_5 &= 0, \\ 2(c_6 - c_5) &= \frac{-N_C M_V}{64\pi^2 F_\pi}, \\ c_1 - c_2 - 8c_3 + c_5 &= 0, \\ d_1 + 8d_2 - d_3 &= \frac{1}{16}, \\ d_3 &= \frac{-N_C M_V^2}{128\pi^2 F_\pi^2} + \frac{1}{16}, \\ G_V &= \frac{F_\pi}{\sqrt{2}}, \\ F_V &= \sqrt{2}F_\pi, \\ F_A &= F_\pi, \\ \lambda' &= \frac{1}{2}, \\ \lambda'' &= 0, \\ \lambda_0 &= \frac{1}{8}. \end{aligned} \tag{28}$$

In numerical evaluations, we will take $M_V = 775$ MeV.

In order to estimate the error of our predictions, we may be conservative and consider uncorrelated variations of the above relations [Eq. (28)] of around $1/3$. Comparison to hadronic tau decay data suggests, however, that the typical

[4]This conclusion is supported by the analysis of the $\tau^- \to K^- \eta \nu_\tau$ decays [41].

TABLE I. The central values of the different contributions to the branching ratio of the $\tau^- \to \pi^- \nu_\tau \ell^+ \ell^-$ decays ($\ell = e, \mu$) are displayed on the left-hand side of the table. The error bands of these branching fractions are given in the right-hand side of the table. The error bar of the IB contribution stems from the uncertainties on the F_π decay constant and τ lepton lifetime [5].

	$\ell = e$	$\ell = \mu$	$\ell = e$	$\ell = \mu$
IB	1.461×10^{-5}	1.600×10^{-7}	$\pm 0.006 \times 10^{-5}$	$\pm 0.007 \times 10^{-7}$
$IB - V$	-2×10^{-8}	1.4×10^{-8}	$[-1 \times 10^{-7}, 1 \times 10^{-7}]$	$[-4 \times 10^{-9}, 4 \times 10^{-8}]$
$IB - A$	-9×10^{-7}	1.01×10^{-7}	$[-3 \times 10^{-6}, 2 \times 10^{-6}]$	$[-2 \times 10^{-7}, 6 \times 10^{-7}]$
VV	1.16×10^{-6}	6.30×10^{-7}	$[4 \times 10^{-7}, 4 \times 10^{-6}]$	$[1 \times 10^{-7}, 3 \times 10^{-6}]$
AA	2.20×10^{-6}	1.033×10^{-6}	$[1 \times 10^{-6}, 9 \times 10^{-6}]$	$[2 \times 10^{-7}, 6 \times 10^{-6}]$
$V - A$	2×10^{-10}	-5×10^{-11}	$\sim 10^{-10}$	$\sim 10^{-10}$
Total	1.710×10^{-5}	1.938×10^{-6}	$(1.7^{+1.1}_{-0.3}) \times 10^{-5}$	$[3 \times 10^{-7}, 1 \times 10^{-5}]$

error of our approach is smaller [44], $\lesssim 20\%$, and we will take this figure for estimating the error ranges. We will, nonetheless, keep $c_1 - c_2 + c_5 = 0$ to avoid the leading powers violating the asymptotic behavior [45]. In this way, we will assume variations of $\pm 20\%$ for the nonvanishing combinations of couplings in Eq. (28): $c_6 - c_5$, $d_1 + 8d_2 - d_3$, d_3, G_V, F_V, F_A, λ' and λ_0, and we will set $|c_1 + c_2 + 8c_3 - c_5| \leq 0.01$ and $|\lambda''| \leq 0.04$ so that they are smaller than analogous nonvanishing couplings according to Eq. (28).

V. PHENOMENOLOGICAL ANALYSIS

Using the results of previous sections, we have evaluated the branching fractions and the invariant-mass spectrum of the $\ell^+\ell^-$ pair for the decays $\tau^- \to \pi^- \nu_\tau \ell^+ \ell^-$ ($\ell = e, \mu$). In order to assess the contributions of structure-dependent (SD) and inner-bremsstrahlung (IB) contributions, we have evaluated separately the moduli squared and interferences in both observables, as discussed in Sec. II. The form factors that describe SD contributions were given in Eqs. (10) to (20), and the coupling constants involved were fixed using short-distance QCD constraints in Eq. (28). The branching ratios that are predicted using these form factors are shown in the second and third columns of Table I; the corresponding allowed ranges that are obtained by letting the couplings vary within 20% of their central values, as described in the previous section, are shown in the fourth and fifth columns of Table I. The couplings which were predicted to vanish ($c_1 + c_2 + 8c_3 - c_5$ and λ'') have a marginal influence on the error estimates. Also, the impact of the variations on λ_0, λ' and on $d_1 + 8d_2 - d_3$ are rather mild and the error ranges are basically determined by the uncertainties on the remaining couplings: F_V, F_A, G_V, $c_5 - c_6$ and d_3.

The normalized invariant-mass distribution of the lepton pair,

$$\frac{1}{\Gamma_\tau} \cdot \frac{d\Gamma(\tau^- \to \pi^- \nu_\tau e^+ e^-)}{ds_{34}}, \tag{29}$$

is shown in Fig. 4. As can be observed, the IB contribution dominates the spectrum for values of $s_{34} \lesssim 0.1$ GeV^2. For larger values (which can be better appreciated in Fig. 5), the SD part overcomes the former, and the AA contribution dominates in the rest of the spectrum, apart from the $\rho(770)$ peak region, where the VV part overtakes it. The interference terms $IB - V$ and $IB - A$ are negative for most of the spectrum and do not appear in the figure.

The normalized $\mu^+\mu^-$ invariant-mass distribution [by a definition similar to Eq. (29)] is shown in Fig. 6. In this case, the IB and SD contributions [essentially AA apart from the $\rho(770)$ peak region] are comparable for $s_{34} \lesssim 0.1$ GeV^2. For higher values of the squared photon-invariant mass, the main contribution comes from the AA part, and the VV contribution shows up through the peak at the $\rho(770)$ mass.

In Figs. 4–6, vertical fluctuations can be appreciated in certain energy regions of the normalized invariant-mass distributions. In order to compute these distributions in the s_{34} variable, we have integrated numerically the decay probability over the remaining four independent kinematical variables by using a FORTRAN code based on the VEGAS routine. The observed fluctuations arise from the Monte Carlo evaluation over the four-body phase-space integration. The branching fractions shown in Table I were

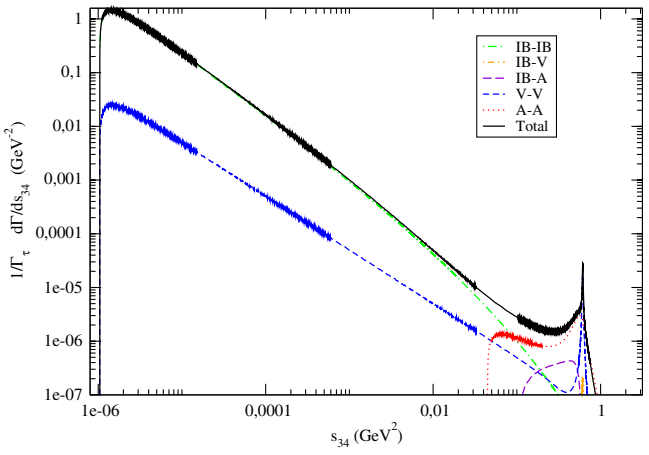

FIG. 4 (color online). The different contributions to the normalized e^+e^- invariant-mass distribution defined in Eq. (29) are plotted. A double logarithmic scale was needed.

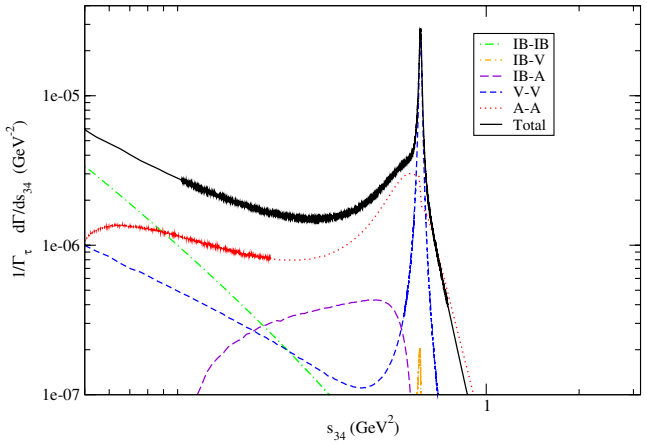

FIG. 5 (color online). The different contributions to the normalized e^+e^- invariant-mass distribution defined in Eq. (29) are plotted in a magnification for $s_{34} \gtrsim 0.1$ GeV^2 chosen to better appreciate the SD contributions. A double logarithmic scale was needed.

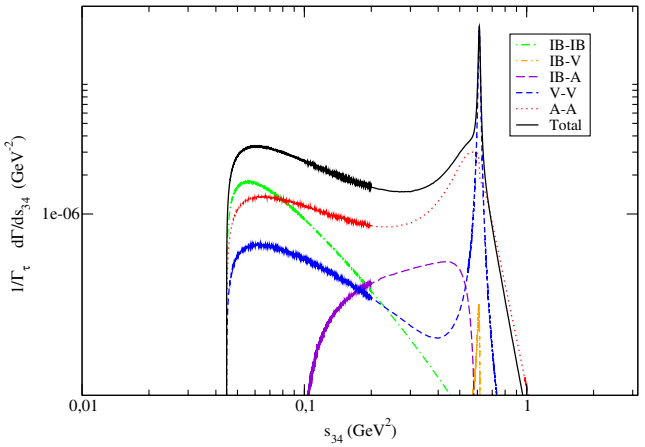

FIG. 6 (color online). The different contributions to the normalized $\mu^+\mu^-$ invariant-mass distribution are plotted. A double logarithmic scale allows the different contributions to be displayed more clearly.

obtained by integrating numerically these invariant-mass distributions and checked by a direct integration over the five independent kinematical variables.

We have found that the SD contribution is sizable (15%) in the case of $\ell = e$ decays and dominant (92%) for $\ell = \mu$. Accordingly, it will be easy to pin it down from the experimental data if enough statistics are accumulated: in $\ell = e$ decays by confirming that the differential decay width ceases to decrease as expected from IB around $s_{34} \sim 0.1$ GeV^2 and starts increasing up to the $\rho(770)$ peak region; and in the $\ell = \mu$ case first because it falls slower than expected from a QED contribution[5] and second, from $s_{34} \sim 0.3$ GeV^2 on, because it starts to rise up to the $\rho(770)$ peak region. In case a fine binning is achieved in this zone, it will be possible to confirm the expected VV contribution in either decay mode as well.

The fact that in both decays the contribution to the decay width of the $s_{34} > 1$ GeV^2 region is negligible justifies our assumption of including only the lightest multiplet of vector and axial-vector resonances. This result is not trivial in the axial-vector case, and in the vector case it is not modified even if the $\rho(1450)$ exchange is included phenomenologically [20].

We have also assessed the relevance of the axial-vector B form factor, introduced in Eq. (3) [see also Eq. (16)]. We find it important, as the $(AA) + (IB - A)$ contributions drop to 33% and 25% of the values shown in Table I if this form factor is neglected. This, in turn, results in a decrease of the branching ratio of 5% for $\ell = e$ and 44% for $\ell = \mu$. Therefore, it is essential to include this contribution in the muon decay channel. This explains why the AA normalized invariant-mass distribution was peaked in the $\rho(770)$ mass region for either channel, since the B form factor is proportional to the isovector component of the electromagnetic dipion form factor.

A future study of the data corresponding to the SD-dominated part of the spectrum will also allow us to test the hadronization proposed in Ref. [9] for the $\tau^- \to \pi^-\gamma\nu_\tau$ decays. In particular, in that reference it was found that

$$\Gamma(\tau^- \to \pi^-(\gamma)\nu_\tau) = \Gamma(\tau^- \to \pi^-\nu_\tau)(1 + \delta_\gamma), \qquad (30)$$

with $\delta_\gamma \sim 1.460 \times 10^{-2}$ for a photon energy threshold of 50 MeV. The SD part, whose contribution was found to be $\delta_\gamma \sim 0.138 \times 10^{-2}$, could be tested through the $\tau^- \to \pi^-\nu_\tau\ell^+\ell^-$ ($\ell = e,\ \mu$) decays considered in this paper. This knowledge can also be extended to the computation of the radiative corrections to the ratio $R_{\tau/\pi} := \Gamma(\tau^- \to \pi^-\nu_\tau)/\Gamma(\pi^- \to \mu^-\bar{\nu}_\mu)$ [8], relevant for lepton universality tests [1].

Finally, the study of radiative tau decays is also important for a faithful modeling of backgrounds in lepton flavor violation searches, as was noted for the $\tau^- \to \pi^-\gamma\nu_\tau$ decays in the case in which the pion is misidentified as a muon and resembles the $\tau^- \to \mu^-\gamma$ [46] signal. The standard simulation of the radiative decay is performed with PHOTOS [47], which only includes the scalar QED contribution, neglecting the SD parts. Analogously, the $\tau^- \to \pi^-\ell^+\ell^-\nu_\tau$ ($\ell = e,\ \mu$) decays under consideration might also mimic the $\tau^- \to \mu^-\ell^+\ell^-$ processes. Although it seems that the inclusion of QCD contributions for the $\ell = \mu$ case will be important (as the SD part gives the bulk of the branching ratio), a devoted study is needed to confirm this, because the involved processes are three- and

[5]The $(1/\Gamma)d\Gamma/ds_{34}$ distribution and the IB contribution to it can be well approximated by $a + b\ \mathrm{Log}(s_{34})$ in the range $[0.11, 0.19]$ GeV^2. We find $b^{\mathrm{TOT}} = -1.314(3) \times 10^{-6}$ and $b^{IB} = -8.87(3) \times 10^{-7}$, quantifying the effect of SD contributions in this region. We quote for completeness our results $a^{\mathrm{TOT}} = -5.63(6) \times 10^{-7}$ and $a^{IB} = -1.221(5) \times 10^{-6}$.

four-body decays, which complicates things with respect to the study in Ref. [46], where the kinematics of $\tau^- \to \mu^- \gamma$ is completely fixed, selecting the photons with almost maximal energy in $\tau^- \to \pi^- \gamma \nu_\tau$ decays as the relevant background.

VI. CONCLUSIONS

We have studied for the first time the $\tau^- \to \pi^- \nu_\tau \ell^+ \ell^-$ ($\ell = e,\ \mu$) decays. We have evaluated the model-independent contributions by using QED and have obtained the structure-dependent part ($W^* \to \pi^- \gamma^*$ vertex) using RχT. This approach ensures the low-energy limit of χPT and includes the lightest resonances as active degrees of freedom worked out within the convenient antisymmetric tensor formalism. We have been able to predict all the couplings involved in the relevant Lagrangian term using short-distance QCD constraints (in the $N_C \to \infty$ limit and restricting the spectrum to the lowest-lying spin-1 resonances) on the related Green functions and form factors, and we have considered the error stemming from this procedure in a conservative way.

Within this framework, we predict $\mathrm{BR}(\tau^- \to \pi^- \nu_\tau e^+ e^-) = (1.7^{+1.1}_{-0.3}) \times 10^{-5}$ and $\mathrm{BR}(\tau^- \to \pi^- \nu_\tau \mu^+ \mu^-) \in [3 \times 10^{-7}, 1 \times 10^{-5}]$. We find that while the $\ell = e$ decays should be within discovery reach at the future superflavor facilities, this will only be possible for the $\ell = \mu$ decays if they happen to be close to the upper limit of the range we have given. The studied hadronic currents are ready for installation in the RχT-based version [22,48] of TAUOLA, the standard Monte Carlo generator for tau lepton decays.

ACKNOWLEDGMENTS

This work has been partially supported by the Spanish Grant No. FPA2011-25948 and Conacyt (México). P. R. acknowledges the hospitality of Departamento de Física at CINVESTAV, where part of this work was done.

APPENDIX

We collect in this appendix the results of summing over polarizations and averaging over that of the tau the different contributions to the squared matrix element. We refrain from writing the lengthy outcome of the contraction of the indices which was used in our programs.

$$
\begin{aligned}
\overline{|\mathcal{M}_{IB}|^2} &= 16 G_F^2 |V_{ud}|^2 \frac{e^4}{k^4} F_\pi^2 M_\tau^2 \ell_{\mu\nu} \Bigg[\frac{-\tau^{\mu\nu} k^2}{(k^2 - 2k\cdot p_\tau)^2} + \frac{4 p^\mu q^\nu k\cdot p_\tau}{(k^2 + 2k\cdot p)(k^2 - 2k\cdot p_\tau)} + \frac{4 p_\tau^\mu q^\nu k\cdot p_\tau}{(k^2 - 2k\cdot p_\tau)^2} \\
&\quad - \frac{2 g^{\mu\nu} k\cdot p_\tau k\cdot q}{(k^2 - 2k\cdot p_\tau)^2} - \frac{4 p^\mu p_\tau^\nu k\cdot q}{(k^2 + 2k\cdot p)(k^2 - 2k\cdot p_\tau)} - \frac{4 p_\tau^\mu p_\tau^\nu k\cdot q}{(k^2 - 2k\cdot p_\tau)^2} + \frac{8 p^\mu p_\tau^\nu p_\tau\cdot q}{(k^2 + 2k\cdot p)(k^2 - 2k\cdot p_\tau)} \\
&\quad + \frac{4 p^\mu p^\nu p_\tau\cdot q}{(k^2 + 2k\cdot p)^2} + \frac{4 p_\tau^\mu p_\tau^\nu p_\tau\cdot q}{(k^2 - 2k\cdot p_\tau)^2} \Bigg], \\
\overline{2\Re e[\mathcal{M}_{IB}\mathcal{M}_V^*]} &= -32 G_F^2 |V_{ud}|^2 \frac{e^4}{k^4} F_\pi M_\tau^2 \Im m\{F_V^*(p\cdot k, k^2) \ell^\mu_{\nu'} \epsilon^{\mu'\nu'\rho'\sigma'} k_{\rho'} p_{\sigma'} \mathcal{V}_{\mu\mu'}\}, \\
\overline{2\Re e[\mathcal{M}_{IB}\mathcal{M}_A^*]} &= -64 G_F^2 |V_{ud}|^2 \frac{e^4}{k^4} F_\pi M_\tau^2 \ell_\mu^{\nu'} \Re e[\mathcal{A}^*_{\mu'\nu'} \mathcal{V}^{\mu\mu'}], \\
\overline{|\mathcal{M}_V|^2} &= 16 G_F^2 |V_{ud}|^2 \frac{e^4}{k^4} |F_V(p\cdot k, k^2)|^2 \epsilon_{\mu'\nu'\rho'\sigma'} \epsilon_{\mu\nu\rho\sigma} k^\rho p^\sigma k^{\rho'} p^{\sigma'} \ell^{\nu\nu'} \tau^{\mu\mu'}, \\
\overline{|\mathcal{M}_A|^2} &= 64 G_F^2 |V_{ud}|^2 \frac{e^4}{k^4} \ell_{\nu\nu'} \tau_{\mu\mu'} \mathcal{A}^{\mu\nu} \mathcal{A}^{\mu'\nu'*}, \\
\overline{2\Re e[\mathcal{M}_V\mathcal{M}_A^*]} &= -64 G_F^2 |V_{ud}|^2 \frac{e^4}{k^4} \Im m[F_V(p\cdot k, k^2) \epsilon_{\mu\nu\rho\sigma} k^\rho p^\sigma \ell^\mu_{\nu'} \tau^{\mu\mu'} \mathcal{A}^{\nu'*}_{\mu'}],
\end{aligned}
\tag{A1}
$$

where we have defined

$$
\begin{aligned}
\ell^{\mu\nu} &= p_-^\mu p_+^\nu + p_-^\nu p_+^\mu - g^{\mu\nu}(m_\ell^2 + p_-\cdot p_+), \qquad \tau^{\mu\nu} = p_\tau^\mu q^\nu + p_\tau^\nu q^\mu - g^{\mu\nu} p_\tau\cdot q, \\
\mathcal{A}^{\mu\nu} &= F_A(p\cdot k, k^2)[(k^2 + p\cdot k) g^{\mu\nu} - k^\mu p^\nu] + B(k^2) k^2 \Bigg[g^{\mu\nu} - \frac{(p+k)^\mu p^\nu}{k^2 + 2p\cdot k} \Bigg], \\
\mathcal{V}_{\mu\nu} &= \frac{2 p_\mu q_\nu}{2k\cdot p + k^2} + \frac{-g_{\mu\nu} k\cdot q + 2 q_\nu p_{\tau\mu} - i\epsilon_{\mu\nu\rho\sigma} k^\rho q^\sigma + k_\nu q_\mu}{k^2 - 2k\cdot p_\tau},
\end{aligned}
\tag{A2}
$$

and used the conservation of the electromagnetic currents, implying $k_\mu \ell^{\mu\nu} = 0 = \ell^{\mu\nu} k_\nu$.

[1] A. Pich, arXiv:1301.4474.
[2] C. Dib, J. C. Helo, M. Hirsch, S. Kovalenko, and I. Schmidt, Phys. Rev. D **85**, 011301 (2012).
[3] D. A. Bryman, P. Depommier, and C. Leroy, Phys. Rep. **88**, 151 (1982).
[4] A. Kersch and F. Scheck, Nucl. Phys. **B263**, 475 (1986).
[5] J. Beringer *et al.* (Particle Data Group), Phys. Rev. D **86**, 010001 (2012).
[6] J. Bijnens, G. Ecker, and J. Gasser, Nucl. Phys. **B396**, 81 (1993).
[7] L. Ametller, J. Bijnens, A. Bramon, and F. Cornet, Phys. Lett. B **303**, 140 (1993); J. Bijnens and P. Talavera, Nucl. Phys. **B489**, 387 (1997); C. Q. Geng, I.-L. Ho, and T. H. Wu, Nucl. Phys. **B684**, 281 (2004); V. Mateu and J. Portolés, Eur. Phys. J. C **52**, 325 (2007); C.-H. Chen, C.-Q. Geng, and C.-C. Lih, Phys. Rev. D **83**, 074001 (2011); D. G. Dumm, S. Noguera, and N. N. Scoccola, Phys. Lett. B **698**, 236 (2011); Phys. Rev. D **86**, 074020 (2012).
[8] A. Sirlin, Nucl. Phys. **B196**, 83 (1982); R. Decker and M. Finkemeier, Phys. Lett. B **316**, 403 (1993); Nucl. Phys. **B438**, 17 (1995); Phys. Lett. B **334**, 199 (1994).
[9] Z.-H. Guo and P. Roig, Phys. Rev. D **82**, 113016 (2010).
[10] J. P. Miller, E. de Rafael, and B. L. Roberts, Rep. Prog. Phys. **70**, 795 (2007); J. Prades, E. de Rafael, and A. Vainshtein, in *Lepton Dipole Moments*, Advanced Series on Directions in High Energy Physics Vol. 20 (World Scientific, Singapore, 2009), pp. 303–318; F. Jegerlehner and A. Nyffeler, Phys. Rep. **477**, 1 (2009).
[11] G. Ecker, J. Gasser, A. Pich, and E. de Rafael, Nucl. Phys. **B321**, 311 (1989).
[12] G. Ecker, J. Gasser, H. Leutwyler, A. Pich, and E. de Rafael, Phys. Lett. B **223**, 425 (1989); V. Cirigliano, G. Ecker, M. Eidemuller, R. Kaiser, A. Pich, and J. Portolés, Nucl. Phys. **B753**, 139 (2006); K. Kampf and J. Novotny, Phys. Rev. D **84**, 014036 (2011).
[13] A. Flores-Tlalpa and G. López Castro (unpublished); See also A. Flores-Tlalpa, G. L. Castro, and G. T. Sánchez, Phys. Rev. D **72**, 113003 (2005).
[14] S. Weinberg, Physica (Amsterdam) **96A**, 327 (1979); J. Gasser and H. Leutwyler, Ann. Phys. (N.Y.) **158**, 142 (1984); Nucl. Phys. **B250**, 465 (1985); J. Bijnens, G. Colangelo, and G. Ecker, J. High Energy Phys. 02 (1999) 020; J. Bijnens, L. Girlanda, and P. Talavera, Eur. Phys. J. C **23**, 539 (2002).
[15] G. 't Hooft, Nucl. Phys. **B72**, 461 (1974); **B75**, 461 (1974); E. Witten, Nucl. Phys., **B160**, 57 (1979).
[16] V. Cirigliano, G. Ecker, H. Neufeld, and A. Pich, J. High Energy Phys. 06 (2003) 012.
[17] P. D. Ruiz-Femenía, A. Pich, and J. Portolés, J. High Energy Phys. 07 (2003) 003.
[18] D. G. Dumm, A. Pich, and J. Portolés, Phys. Rev. D **69**, 073002 (2004).
[19] D. G. Dumm, A. Pich, and J. Portolés, Phys. Rev. D **62**, 054014 (2000).
[20] D. G. Dumm, P. Roig, A. Pich, and J. Portolés, Phys. Lett. B **685**, 158 (2010).
[21] D. G. Dumm, P. Roig, A. Pich and J. Portolés, Phys. Rev. D **81**, 034031 (2010).
[22] I. M. Nugent, T. Przedzinski, P. Roig, O. Shekhovtsova, and Z. Was (to be published); We used the improved results, updating O. Shekhovtsova, I. M. Nugent, T. Przedzinski, P. Roig, and Z. Was, arXiv:1301.1964.
[23] I. M. Nugent, arXiv:1301.7105.
[24] F. Guerrero and A. Pich, Phys. Lett. B **412**, 382 (1997).
[25] J. Gasser and U. G. Meissner, Nucl. Phys. **B357**, 90 (1991).
[26] J. Bijnens, G. Colangelo, and P. Talavera, J. High Energy Phys. 05 (1998) 014.
[27] J. Bijnens and P. Talavera, J. High Energy Phys. 03 (2002) 046.
[28] J. J. Sanz-Cillero and A. Pich, Eur. Phys. J. C **27**, 587 (2003).
[29] P. Roig, Nucl. Phys. B, Proc. Suppl., NUPHBP14263 (2012) 161.
[30] A. Pich and J. Portolés, Phys. Rev. D **63**, 093005 (2001).
[31] J. F. De Trocóniz and F. J. Ynduráin, Phys. Rev. D **65**, 093001 (2002).
[32] B. Ananthanarayan, I. Caprini, and I. S. Imsong, Phys. Rev. D **83**, 096002 (2011).
[33] C. Hanhart, Phys. Lett. B **715**, 170 (2012).
[34] D. G. Dumm and P. Roig, arXiv:1301.6973 (to be published).
[35] D. R. Boito, R. Escribano, and M. Jamin, Eur. Phys. J. C **59**, 821 (2009).
[36] B. Aubert *et al.* (*BABAR* Collaboration), Phys. Rev. Lett. **103**, 231801 (2009).
[37] E. G. Floratos, S. Narison, and E. de Rafael, Nucl. Phys. **B155**, 115 (1979).
[38] M. Jamin, A. Pich, and J. Portolés, Phys. Lett. B **640**, 176 (2006).
[39] M. Jamin, A. Pich, and J. Portolés, Phys. Lett. B **664**, 78 (2008).
[40] D. R. Boito, R. Escribano, and M. Jamin, J. High Energy Phys. 09 (2010) 031.
[41] R. Escribano, S. González-Solís, and P. Roig (unpublished).
[42] V. Cirigliano, G. Ecker, M. Eidemuller, A. Pich, and J. Portolés, Phys. Lett. B **596**, 96 (2004).
[43] S. Weinberg, Phys. Rev. Lett. **18**, 507 (1967).
[44] P. Roig, I. M. Nugent, T. Przedzinski, O. Shekhovtsova, and Z. Was, AIP Conf. Proc. **1492**, 57 (2012).
[45] D. G. Dumm and P. Roig, Phys. Rev. D **86**, 076009 (2012).
[46] Z.-H. Guo and P. Roig, Nucl. Phys. B, Proc. Suppl. **218**, 122 (2011).
[47] E. Barberio, B. van Eijk, and Z. Was, Comput. Phys. Commun. **66**, 115 (1991); E. Barberio and Z. Was, Comput. Phys. Commun. **79**, 291 (1994); P. Golonka, B. Kersevan, T. Pierzchala, E. Richter-Was, Z. Was, and M. Worek, Comput. Phys. Commun. **174**, 818 (2006); P. Golonka and Z. Was, Eur. Phys. J. C **45**, 97 (2006); N. Davidson, T. Przedzinski, and Z. Was, arXiv:1011.0937.
[48] O. Shekhovtsova, T. Przedzinski, P. Roig, and Z. Was, Phys. Rev. D **86**, 113008 (2012).